A Framework for Dispatching of an Electric Vehicle Fleet using Vehicle-to-Grid Technology

Abdullah Kürşat Aktar[1], Akın Taşcıkaraoğlu[1,*], Sırrı Sunay Gürleyük[1], João P. S. Catalão[2]

[1]*Electrical and Electronics Engineering Department, Mugla Sitki Kocman University, Mugla, Turkey*
[2]*Faculty of Engineering of the University of Porto and INESC TEC, Porto 4200-465, Portugal*
** akintascikaraoglu@mu.edu.tr*

Abstract

Future planning of the energy supply and transportation should be taken into consideration simultaneously. The cooperation of related stakeholders, especially institutions, distribution companies and new technology developers is of great importance in terms of foreseeing and preventing the problems to be encountered and of benefiting together. As it becomes more challenging to maintain the balance between energy supply and demand in electric power systems due to the stochasticity of both load demands and renewable power generation, Electric Vehicle (EV) batteries can play a critical role in supporting this balance for a given period. In this study, an optimization algorithm based on mixed integer linear programming is used to evaluate the economic and technical benefits of EVs when they are used as mobile energy storage systems by system operators, which is called the concept of "Vehicle for Grid" (VfG). It is particularly aimed to alleviate the load demand on grid during the peak energy periods. The results obtained for two types of EVs with different characteristics show that the economic and operational benefits can be maximized when the optimum number and specification of EVs to be integrated into the system are determined. In the best-case scenario in which 15 EVs each with a capacity of 200 kWh are used, the peak-to-average power ratio of the load curve decreases by 6.56%.

Keywords: Electric vehicle, fleet management, mobile energy storage, peak shaving, vehicle for grid.

Nomenclature

The abbreviations, sets, parameters and variables used in this paper are alphabetically listed below.

A. Abbreviations

ED	Energy Drawn.
ESS	Energy Storage System.
EV	Electric Vehicle.
RES	Renewable Energy Source.

SOE	State-of-Energy.
VfG	Vehicle for Grid.
$V2G$	Vehicle to Grid.

B. Sets

B_l^{ij}	Index of sending end i buses and receiving end j buses.
EV	Index of electrical vehicles.
i	Index of buses.
l	Index of lines.
t	Index of time interval for energy flow.
tt	Index of time interval for travel of EV.
v	Index of EV velocity.

C. Parameters

A	Vehicle frontal area [m^2].
B_l	Susceptance of line l [pu].
C_d	Aerodynamic drag coefficient.
C_{rr}	Coefficient of rolling resistance.
CE^{ESS}	Charging efficiency of the ESS battery.
CE^{EV}	Charging efficiency of the EV battery.
CS	Number of charging and discharging socket of buses.
DE^{ESS}	Discharging efficiency of the ESS.
DE^{EV}	Discharging efficiency of the EV battery.
EC^{EV}	Energy consumption of EV [kWh].
$F_{v,tt}^{a}$	Aerodynamic drag force of EV in time interval tt [kg.m/s^2].
$F_{v,tt}^{ac}$	Acceleration force of EV in time interval tt [kg.m/s^2].
F_{tt}^{g}	Gravity force of EV in time interval tt [kg.m/s^2].
F_{tt}^{r}	Rolling friction force of EV in time interval tt [kg.m/s^2].
$F_{v,tt}^{t}$	Total traction force of EV in time interval tt [kg.m/s^2].
f_m	Mass factor.
g	Gravity of earth [m/s^2].
M^{EV}	Mass of EV [kg].
$M_{i,l}^{F}$	Coefficient is 1 if line l of bus i is receiving end; 0 if line l of bus i is sending end; 0 if it is not both.
$M_{i,l}^{L}$	Coefficient is 1 if line l of bus i is sending end; 0 if it is not.
$M_{l,i}^{W}$	Coefficient that belongs to bus i and line l is obtained from transpose of $M_{i,l}^{F}$ matrix.
N	Sufficiently large positive constant.
$P_{v,tt}^{ve}$	Electrical power demand of EV in time interval tt [W].
$P_{v,tt}^{vm}$	Mechanical power demand of EV in time interval tt [W].
$P_{i,t}^{L,total}$	Active power demand of bus i in time interval t [pu].
$Q_{i,t}^{L}$	Reactive power demand of bus i in time interval t [pu].
$R_i^{ESS,\mathrm{ch}}$	Charging rate limit of ESS that is connected to bus i [kW].
$R_i^{ESS,dis}$	Discharging rate limit of ESS that is connected to bus i [kW].
$R_i^{EV,\mathrm{ch}}$	Charging rate limit of EV that is connected to bus i [kW].

$R_i^{EV,dis}$ Discharging rate limit of EV that is connected to bus i [kW].
R_l Resistance of line l [pu].
$SOE_i^{ESS,ini}$ Initial SOE of the ESS that is connected to bus i [kWh].
$SOE_i^{ESS,max}$ Maximum SOE of the ESS that is connected to bus i [kWh].
$SOE_i^{ESS,min}$ Minimum SOE of the ESS that is connected to bus i [kWh].
$SOE_{i,j,m}^{EV,ini}$ Initial SOE of the EV [kWh].
$SOE_{i,j,m}^{EV,max}$ Maximum SOE of the EV [kWh].
$SOE_{i,j,m}^{EV,min}$ Minimum SOE of the EV [kWh].
V_{max} Permitted maximum voltage level of buses [pu].
V_{min} Permitted minimum voltage level of buses [pu].
$V_{v,tt}^{EV}$ EV speed [m/s].
$V_{v,tt}^{W}$ Wind speed [m/s].
X_l Reactance of line l [pu].
α Acceleration [m^2/s].
η_d Driving efficiency.
ρ Air density [kg/m^3].
θ Road slope angle [°].
$\Delta L_{j,m}$ Distance to point j through route m [km].
ΔT Time period [min].

D. Variables

$m_{i,t}^{EV}$ Binary variable (1 if the EV is connected to bus i in time interval t; 0 otherwise).
$P_{i,t}^{G}$ Total active power of bus i in time interval t [pu].
$P_{i,t}^{L}$ Total power demand of bus i in time interval t [pu].
$P_{i,t}^{S}$ Total power flowing from transformer to bus i in time interval t [pu].
$P_{i,t}^{ESS,ch}$ Charging power by ESS that is connected to bus i in time interval t [kWh].
$P_{i,t}^{ESS,dis}$ Discharging power by ESS that is connected to bus i in time interval t [kWh].
$P_{i,t}^{EV,ch}$ Charging power by EV that is connected to bus i in time interval t [kWh].
$P_{i,t}^{EV,dis}$ Discharging power by EV that is connected to bus i in time interval t [kWh].
$P_{l,t}^{\text{loss}}$ Total active power loss of line l in time interval t [pu].
$\hat{P}_{l,t}^{\text{loss}}$ Model variable to represent total active power loss of line l in time interval t [pu].
$P_{l,t}^{r}$ Total active power of line l in time interval t [pu].
$Q_{l,t}^{\text{loss}}$ Total reactive power loss of line l in time interval t [pu].
$Q_{i,t}^{G}$ Total reactive power of bus i in time interval t [pu].
$Q_{l,t}^{r}$ Total reactive power of line l in time interval t [pu].
$SOE_{i,t}^{ESS}$ SOE of the ESS is connected to bus i in time interval t [kWh].
$SOE_{i,t}^{EV}$ SOE of the EV battery is connected to bus i in time interval t [kWh].
$u_{i,t}^{ch}$ Binary variable (-1 if the EV is charging in time interval t; 0 otherwise).
$V_{i,t}$ Voltage magnitude of bus i in time interval t [pu].
$W_{i,t}$ Equivalent of cosine term of power flow equation on line (i,j) in time interval t [pu].
$W_{r,t}$ Square of voltage magnitude at receiving end bus r $(r \in i)$ in time interval t [pu].

1. Introduction

1.1 Literature Overview

Under the conditions of the Covid-19 pandemic, similar to the other sectors, the electricity sector has deviated from its growth path. With the increase in the normalization rate, it is expected to reach the estimated growth rates rapidly. In meeting the global energy needs, electrical energy is anticipated to continue to rise to the top in the long run. Also, with the increase in the world population, there will be a rise in the necessities, thus it will be necessary to use more electrical energy, especially from the Renewable Energy Sources (RESs). While renewable energy plays an important role in reducing CO_2 emissions, which is one of the most important environmental concerns, it is expected to meet 21% of the world energy consumption in 2030 according to International Energy Agency [1]. Currently, the transportation in the world is provided in two ways: electrical energy and fossil fuel. While the energy demand continues to increase in both cases, the transportation energy demand of non-OECD countries is expected to increase by 77% until 2050 [2]. Besides, the International Energy Outlook shows that global transport sector energy use will increase around 50% between 2012 and 2040 [3].

The electrification of transportation, which has been first started with the hybrid Electric Vehicles (EVs) and continued with the plug-in EVs, is a new situation for the world that has to overcome. The growth in the number of EVs has considerably increased the demanded power in distribution grids at the last decade. Managing the charging operations of EVs has become therefore crucial to avoid grid failures and distribute resources efficiently [4].

When the controlled and uncontrolled charging situations of EVs are compared, it has been clearly revealed that the controlled charging state is much better in terms of losses and overloading [5]. It is, however, obvious that smart charging systems might only provide a temporary solution to the rapidly increasing capacity of EVs. To this end, the Vehicle-to-Grid (V2G) operation, which implies the energy flow from EV battery to grid for a more economic and flexible operation, has come into prominence recently. This technology shows that the need for energy storage and power regulation brought about by the increase in RES can be eliminated by using EV batteries to meet the frequency balancing, power quality and system reliability conditions [6, 7]. In [8], it is mentioned that V2G operations at high charging rates do not cause any negative effects in terms of system reliability and power quality. Moreover, with the simplest use of V2G technology, the difference between the minimum and maximum values in the consumption curve could be easily reduced [9].

The V2G and G2V technologies have the potential to support the sustainability of the distribution systems provided that the necessary improvements in the system infrastructures are implemented. However, the increasing number of EVs with different usage patterns makes the management of the system more challenging [10]. The value and necessity of V2G operations is better understood when it is considered that 30% of the distribution transformers will face overload situation with the increase of 5 kW in

the energy consumption of the houses in Norway [11]. The first work on the V2G concept was done in Japan for the peak shaving and load shifting [12]. A large-scale study was also conducted in [12] for the arbitrage transaction in the UK between 2018 and 2021 with 320 sockets.

It has been stated that 600 GW of capacity can be used flexibly thanks to the V2G operations in various studies conducted in China, India, EU and USA [13]. Being able to use this amount of energy at peak hours may bring many operational advantages. According to the 2030 projection, the total capacity of energy in the EVs batteries will be about 20 TWh, which is equivalent to 27% of the daily global electricity production [14]. The mentioned capacity could be obtained through contracts that can be made in many ways, such as using EVs in V2G operations in exchange for free charging [15].

Energy transfer from an EV to grid does not only provide benefits to network, but also offers opportunities to users who include their EV in the system for this purpose. It can be expressed as an incentive situation to share the EV during the parking time to support the network and gain financial advantages in return [16]. From a different point of view, it has also been put forward that the benefits obtained will increase with the use of EVs not individually but collectively (such as a fleet) in the system, which provides more predictable power management and advanced smart charging systems [17]. The study in [18] showed that profit maximization could be achieved while prioritizing grid stability by performing V2G operations in markets that have different characteristics. In another study, it was aimed to maximize income for both the aggregator and EV owners by creating pools of private and commercial EVs.

In addition, it has been revealed that the differences in the working styles of commercial enterprises with more than one EV such as cargo companies and the usage habits of private EV owners bring opportunity to create mixed pools and have a positive effect on income up to seven times [19]. In another study that supports the same idea, in order to reduce the fluctuations caused by the EVs with high demand and to minimize the operating costs, it was aimed to control the charge-discharge periods of EVs by using the TOU pricing mode. However, the optional participation of EVs in the V2G operation and not being in the system as a fleet limited the exploitation of the EVs in the cost minimization [20]. Besides, in a study that examines seasonal changes, it was stated that the operational benefits might be higher in the winter period with the increase in incentives [21]. In the study aiming to increase the benefits with the coordinated charging operations, the potential impacts of ESS and RES on the benefits have not been considered.

As mentioned above, while the number of EV users involved in the system increases, the system management becomes more challenging. Also, the constraints such as the personal driving preferences of the EV users, the arrival and departure times of the EVs to/from the parking area, and the State-of-Energy (SOE) limitations of the EV battery have an impact on the efficiency of the system management [22]. Nonetheless, the support of an EV fleet on the crucial power system operations such as valley filling and peak shaving was not discussed in [22]. In order to have a more efficient system, the idea of the VfG, which is a new perspective

that takes into account the EVs to be used only in line with the needs of the grid, has been put forward recently in the literature. In a study conducted with the EVs moving between different regions as a fleet owned only by the grid operator, it is stated that an economic management can be achieved by taking the electricity unit price, demand level and SOE of the battery into account [23]. In another study, it was stated that working together to reduce the system losses and operating costs of companies with EVs belonging to generation and distribution companies provides remarkable benefits for both parties [24]. At the same time, it might be possible to reduce the new investment costs with the increase in the system efficiency by the control of peak-energy time. However, the energy consumption of the EVs was not taken into account in [23] and [24], and only the mass movement of the EV fleet was considered in these studies, which might decrease the benefits compared to the case where the fleet can be distributed if necessary.

In this study, unlike the studies mentioned above, an EV fleet, which is free from time and location constraints for the VfG operation, is considered to be deployable to the appropriate bus nodes. Besides, a more effective operation of the electricity grid is aimed with the valley filling and peak shaving applications by taking the energy consumption of EVs into account. The cases with different types and numbers of EVs are examined and also the benefits of including RES and ESSs in the system are investigated.

1.2 Content and Contributions

This study considers an EV fleet including a number of EVs that have the possibility to connect to different buses of the electrical grid. The mobility of EVs provides a more flexible grid management and enables different sizes of capacities to be provided at the bus node according to the demand.

The main aim of the study is to maximize the economic benefits of using an EV fleet while providing the necessary support to the grid. To this end, a strategy based on demand response implementation is proposed where the optimal usage of the energy stored in the EV battery is investigated in order to shave the peak load in the system. At the same time, a loss reduction is accomplished by supplying energy to the closest branch to the consumer.

The contribution of this study is multifaceted:

- The use of the EVs as energy storage units within the scope of VfG is evaluated.
- In order to determine the places and times where and when the EVs will be used, an energy management algorithm is proposed to make the most appropriate decisions as a result of certain comparisons, and it is aimed to make the charging and discharging operations of the EVs in a way that provides the highest economic benefit.
- Considering the fact that the real data are used in the designed system, the benefits of EV technology for the network and the problems to be encountered during real applications create an infrastructure for future research.

1.3 Organization of the Paper

The paper is organized as follows. The developed system is explained in Section 2. Then, the optimization algorithm is tested with different case studies in Section 3. A discussion is provided in Section 4 and finally conclusions and future studies are presented in Section 5.

2. Methodology

In the proposed model, a distribution system with commercial consumers that have different load characteristics is considered. Charging stations that have six charging sockets are located at Low-Voltage (LV) side of the distribution system to serve bidirectional energy flow at each bus node. Transformers at each LV bus node provide energy as the main energy supplier as shown in Fig. 1. Besides, the EV fleet belonging to a Distribution System Operator (DSO) is parked at a parking area for travelling to bus nodes when it is needed. It is assumed that the parking area is at a location where it will be possible to reach all the bus nodes in a reasonable time. Each EV connected to the bus nodes behaves like a stationary ESS. When selecting the bus node to be connected, the optimization algorithm considers the load demand of the bus nodes and the amount of energy required to travel to the relevant nodes. The designed system aims to determine the optimum size and operation of EVs as an energy storage system. The optimization problem and related mathematical expressions are given by Eqs. (1)- (28).

As mentioned above, the main objective of the proposed optimization problem based on mixed integer linear programming is to minimize the Energy Drawn (ED) from the grid via transformer during the peak load period and the energy consumption of EVs to travel bus node described between t_1 and t_2 by Eq. (1). Active and reactive energy flow equations are expressed by (2) and (3). Transformers are the supplier side and commercial facilities and homes are the consumer side of system. The EVs can behave as supplier or consumer using the bidirectional operation modes via charging stations shown by Eqs. (4) and (5). AC power flow Eqs. (6)-(11) taken from [25] represent the system with second order conic programming.

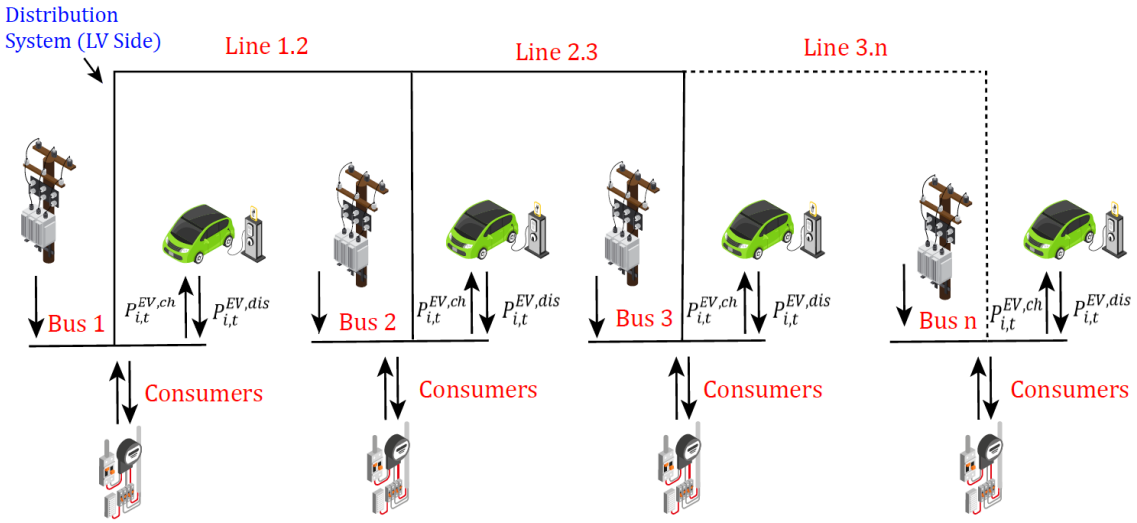

Fig. 1. Block diagram of the distribution system considered.

The rated power limitations of EV charging and discharging are shown by (12) and (13), respectively. The change in the SOE of the EVs when they are connected to the bus node and when they are traveling is calculated by (14) and (15), respectively. Constraint (16) determines the EV battery limitations and initial value of EV battery is defined by Eq. (17).

$$Minimize\ ED = \sum_{t1}^{t2}\sum_{i} P_{i,t}^{S} + \sum_{EV}\sum_{i} EC_{i}^{EV} \tag{1}$$

subject to:

$$P_{i,t}^{G} - P_{i,t}^{L} = \sum_{l\in B_l^{ij}} \left(M_{i,l}^{F}\cdot P_{l,t}^{r} + M_{i,l}^{L}\cdot P_{l,t}^{\text{loss}}\right)\ \forall i,t \tag{2}$$

$$Q_{i,t}^{G} - Q_{i,t}^{L} = \sum_{l\in B_l^{ij}} \left(M_{i,l}^{F}\cdot Q_{l,t}^{r} + M_{i,l}^{L}\cdot Q_{l,t}^{\text{loss}} - B_l\cdot M_{l,i}^{W}\cdot W_{i,t}\right)\ \forall i,t \tag{3}$$

$$P_{i,t}^{G} = P_{i,t}^{EV,dis} + P_{i,t}^{S}\ \forall i,t \tag{4}$$

$$P_{i,t}^{L} = P_{i,t}^{L,total} + P_{i,t}^{EV,\text{ch}}\ \forall i,t \tag{5}$$

$$W_{i,t} = V_{i,t}^{2}\ \forall i,t \tag{6}$$

$$P_{l,t}^{\text{loss}} = 2\cdot R_l\cdot \hat{P}_{l,t}^{\text{loss}}\ \forall l,t \tag{7}$$

$$X_l\cdot P_{l,t}^{\text{loss}} - R_l\cdot Q_{l,t}^{\text{loss}} = 0\ \forall l,t \tag{8}$$

$$\sum_{i}\left(M_{l,i}^{W}\cdot W_{i,t}\right) - 2\cdot\left(R_l\cdot P_{l,t}^{r} + X_l\cdot Q_{l,t}^{r}\right) = R_l\cdot P_{l,t}^{\text{loss}} + X_l\cdot Q_{l,t}^{\text{loss}}\ \forall l,t \tag{9}$$

$$2\cdot \hat{P}_{l,t}^{loss}\cdot W_{r,t} \geq {P_{l,t}^{r}}^{2} + {Q_{l,t}^{r}}^{2}\ \forall l,t \tag{10}$$

$$V_{min}^{2} \leq W_{i,t} \leq V_{max}^{2}\ \forall i,t \tag{11}$$

$$0 \leq P_{i,t}^{EV,\text{ch}} \leq R_i^{EV,\text{ch}}\cdot u_{i,t}^{ch}\ \forall i,t \tag{12}$$

$$0 \leq P_{i,t}^{EV,dis} \leq R_i^{EV,dis}\cdot(1-u_{i,t}^{ch})\ \forall i,t \tag{13}$$

$$\text{SOE}_{\text{i,j,m,t}}^{\text{EV}} = \text{SOE}_{\text{i,j,m,(t-1)}}^{\text{EV}} + \left(\text{CE}^{\text{EV}}\cdot \text{P}_{\text{i,t}}^{\text{EV,ch}} - \frac{\text{P}_{\text{i,t}}^{\text{EV,dis}}}{\text{DE}^{\text{EV}}}\right)\cdot \Delta\text{T}\ \forall \text{t}\ \ \text{if i} = \text{j} \tag{14}$$

$$\text{SOE}_{\text{i,j,m,t}}^{\text{EV}} = \text{SOE}_{\text{i,j,m,(t-1)}}^{\text{EV}} - \text{EC}^{\text{EV}}\cdot \Delta\text{L}_{\text{j,m}}\ \forall \text{t}\ \ \text{if i} \neq \text{j} \tag{15}$$

$$SOE_{i,j,m}^{EV,min} \leq SOE_{i,j,m,t}^{EV} \leq SOE_{i,j,m}^{EV,max}\ \ \forall i,j,m,t \tag{16}$$

$$SOE_{i,j,m,1}^{EV} = SOE_{i,j,m}^{EV,ini}\ \ \forall i,j,m \tag{17}$$

Mathematical model equations to calculate the energy consumption of EVs are described by (18) – (22) [26]. Total traction force $F_{v,tt}^{t}$ consists of four main forces, which are acceleration force, $F_{v,tt}^{ac}$, aerodynamic drag force, $F_{v,tt}^{a}$, rolling friction force, F_{tt}^{r}, and gravity force, F_{tt}^{g}. Mechanical and electrical power needed to move the EVs are expressed by (23) and (24), respectively. Total energy consumption of EV during the driving period can be calculated by (25).

$$F_{v,tt}^{t} = F_{v,tt}^{ac} + F_{v,tt}^{a} + F_{tt}^{r} + F_{tt}^{g}\ \ \forall v,tt \tag{18}$$

$$F_{v,tt}^{a} = \frac{1}{2}.\rho.A.C_d.(V_{v,tt}^{EV} - V_{v,tt}^{W})^2\ \ \forall v,tt \tag{19}$$

$$F_{tt}^{r} = M^{EV}.g.C_{rr}.\cos(\theta)\ \forall tt \tag{20}$$

$$F_{tt}^{g} = M^{EV}.g.\sin(\theta)\ \forall tt \tag{21}$$

$$F_{v,tt}^{ac} = f_{m}.M^{EV}.\alpha\ \forall v,tt \tag{22}$$

$$P_{v,tt}^{vm} = F_{v,tt}^{t}.V_{v,tt}^{EV}\ \forall tt \tag{23}$$

$$P_{v,tt}^{ve} = \frac{P_{v,tt}^{vm}}{\eta_d} \; \forall tt \tag{24}$$

$$EC^{EV} = \sum_{tt} \frac{\left(P_{v,tt}^{ve}.\Delta T\right)}{1000} \tag{25}$$

Eq. (26) ensures that an EV can be connected to only one bus in time interval t. Since each bus has a certain number of connection sockets, the number of EVs that can be connected is limited by Eq. (27). The displacement of the EV in each time interval creates an inefficient situation in terms of both energy consumption and travel time. To have a more efficient operation, the departure of an EV from the bus is prevented by (28). Consequently, the objective function (1) is minimized by considering the constraints (2) - (28).

$$\sum_{i} m_{i,t}^{EV} = 1 \; \forall t, EV \tag{26}$$

$$0 \leq \sum_{EV} m_{i,t}^{EV} \leq CS \; \forall i, t \tag{27}$$

$$m_{i,t}^{EV} - m_{i,(t-1)}^{EV} = 0 \; \forall i, t, EV \; if \; t > 1 \tag{28}$$

The equations of the electrical grid and EV models in the optimization algorithm are given by (1) – (28). The sequential representation of the proposed optimization algorithm consisting of mainly seven steps is presented in Fig 2.

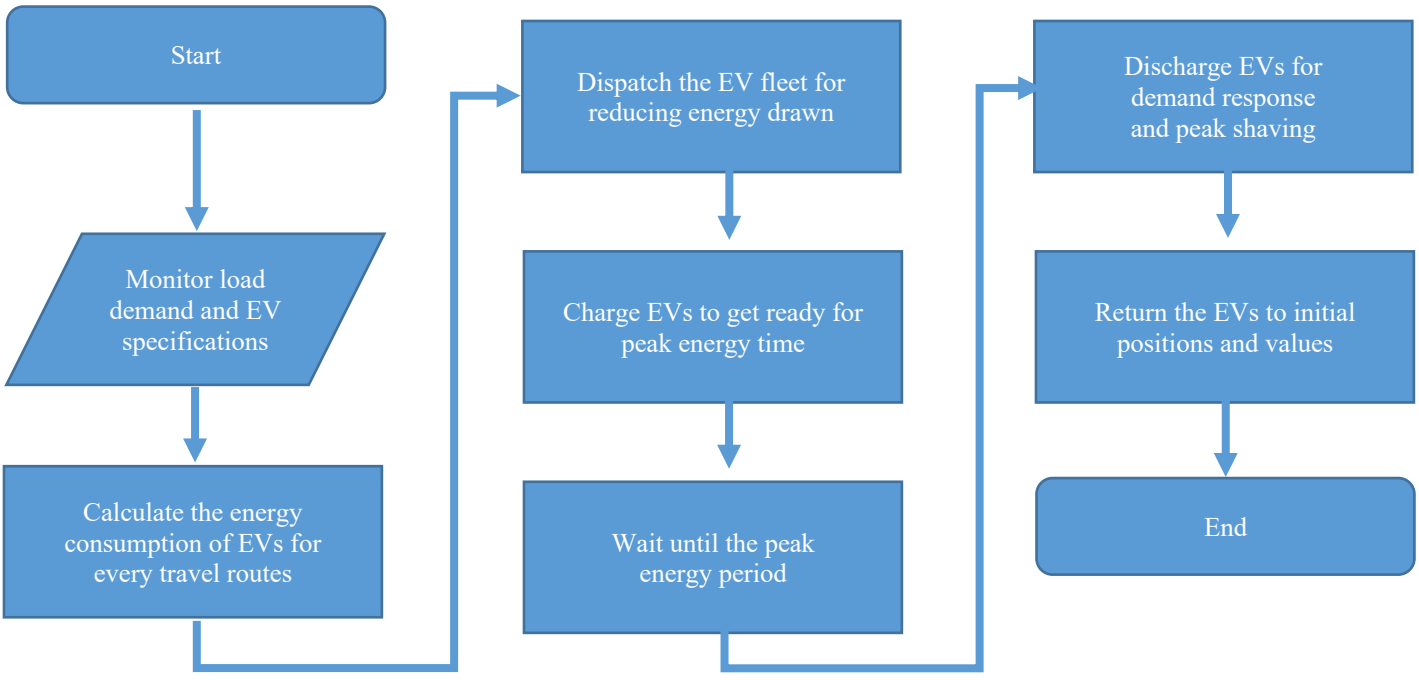

Fig. 2. Sequential representation of the proposed optimization algorithm.

3. Simulation and Results

3.1. Input Data

The data used during the study are as follows. Line parameters of 6 LV buses are given in Table 1. Resistance and reactance values between bus nodes in the table are shown in per unit (pu) values. The base values used are 1 MVA for apparent power, 20 kV for voltage and 400 Ω for impedance.

As a mobile energy source, each EV can move from the parking lot to different connection points. Thus, EV's energy consumption during travel period between parking area and any bus node has to be taken into account to determine the SOE of EV battery. In general, it is possible to find EVs with a wide variety of battery capacities and specific features. In this study, two types of EVs are considered; however, the results of the optimization algorithm for many EVs can be examined with simple changes to the parameters. EV type-1 is considered as any commercial EV and EV type-2 is considered as an EV similar to Tesla Cybertruck Tri Motor, but with a larger battery. The parameters for calculating the energy consumption of EV type-1 and EV type-2 are given in Table 2 [27]. The electrical energy consumption of the EV is calculated by Eq. (18) - (25) using environmental parameters such as wind speed, air density, and the EV-related parameters such as mass and front area.

When an EV is connected to any bus node, it operates as a stationary energy storage system. The energy charge and discharge exchanges occur according to the limitations in Table 3 [28, 29]. Charge - discharge efficiency, and the initial and minimum SOE values of EVs are same for both EV type-1 and EV type-2. EV type-1 has a battery capacity of 100 kWh with 25 kW charging - discharging rate, while EV type-2 has a capacity of 200 kWh with 75 kW charging - discharging rate. Units in the electrical grid model are expressed in pu, while the power units in the EV model are expressed in kW. It should be noted that the related parameters and variables in the power grid model are multiplied by the base power due to the use of pu values.

In this study, the load demand of the consumer for a typical spring day between 09:00 am and 09:00 pm is selected. The data for demand power curves are obtained from a regional distribution company in order to ensure the similarity to the real cases. According to the load profile given in Fig. 3, the charging, discharging and no operation time intervals are selected. EVs are placed in the most suitable locations determined by the algorithm at 09:00 am. After the arrival of EVs to the bus nodes, the EV charging mode is active between 09:00 am and 11:30 am, which is the low energy consumption period, to be ready for the peak shaving operation.

There is no operation between 11:40 am and 2:30 pm so as to use the energy stored in the EV battery efficiently at the peak energy period. At the same time, for avoiding the early battery degradation, the attention is paid to both the discharge period and the minimum SOE of the battery. Therefore, the discharge period is chosen between 2:40pm and 6:40pm, which is also the peak energy period. After the discharge period, it is assumed that the EVs can be recharged or returned to the parking area with the minimum SOE value until the test period ends. Comprehensive evaluations are made on the optimization algorithm by using

different types and numbers of EVs in order to increase the economic and operational benefits. Besides, using an ESS can offer remarkable economic benefits by charging when electricity prices are low and discharging when electricity is expensive. The use of EVs as mobile ESS enables more effective use of the grid thanks to the load shifting operation. The main aim of evaluating the different quantities of EVs in different cases is to reveal the economic and operational benefits on the grid by having opportunity to use different storage capacities.

Table 1. Line parameters of the distribution system considered

Line	From	To	R [pu]	X [pu]
L1	2	1	0.00071	0.00036
L2	3	2	0.00017	0.00009
L3	4	3	0.00153	0.00051
L4	4	5	0.00035	0.00012
L5	5	6	0.00133	0.00044

Table 2. EV parameters used in the calculation of the relevant energy consumption

Parameter	EV Type-1	EV Type-2
Mass	1360 kg	3000 kg
Mass factor	1.05	1.05
Coefficient of rolling resistance	0.02	0.0126
Air density	1.225 kg/m^3	1.225 kg/m^3
Vehicle frontal area	2 m^2	3.4 m^2
Aerodynamic drag coefficient	0.5	0.47
Wind speed	0 m/s	0 m/s
Road slope angle	0 °	0 °
Gravity of Earth	9.8 m/s^2	9.8 m/s^2
Efficiency of EV	0.9	0.9

Table 3. EV & ESS parameters for energy exchange

Parameter	EV Type-1	EV Type-2	ESS
CE^{EV}	0.95	0.95	0.95
DE^{EV}	0.95	0.95	0.95
$R^{EV,\mathrm{ch}}$	25 kW	75 kW	75 kW
$R^{EV,dis}$	25 kW	75 kW	75 kW
$SOE^{EV,ini}$	60 kWh	60 kWh	250 kWh
$SOE^{EV,min}$	25 kWh	25 kWh	50 kWh
$SOE^{EV,max}$	100 kWh	200 kWh	400 kWh

3.2. Results

In order to determine the benefits of the proposed model, five different cases are considered:

- **Case 1:** 15 type-1 EVs are available in the parking lot.
- **Case 2:** 30 type-1 EVs are available in the parking lot.
- **Case 3:** 15 type-2 EVs are available in the parking lot.
- **Case 4:** 30 type-2 EVs are available in the parking lot.
- **Case 5:** 15 type-2 EVs are available in the parking lot. RES and ESS are included.

A time granularity of 10 min (i.e., 0.166 h) is used in all five cases. General Algebraic Modeling System (GAMS) version 25.1.3 is used to test the constrained optimization algorithm and MOSEK solver is used to solve the problem. The average solution time is 0.3 seconds on a 2.21 GHz, quad-core i7-8750H processor PC with 16GB of RAM. The stopping criteria and the iteration limit are chosen 1.0e-6 and 1000000, which are the MOSEK solver's default values, respectively. The algorithm produces the optimal results without reaching the termination limits, which indicates that reliable results are obtained in terms of the accuracy.

In Case 1 and Case 2, the same type of EVs with a maximum capacity of 100 kWh is used for VfG operation. The only difference between these two cases is the number of EVs used. In Case 3 and Case 4, it is assumed that the EV has a capacity of 200 kWh. In these five cases, the benefits of EVs that have different specifications and numbers on the grid supporting operations are investigated. In all cases, it is aimed to optimally reduce the energy drawn from the transformer in the peak energy time interval by connecting the EVs to different buses where the load values of each bus are shown in Fig. 3.

As shown in Fig. 4, Case 1 and Case 2 are effective in stabilizing the energy drawn from the grid during the test period. Between 09:00 am and 11:30 am, it is observed that the load curve moves upwards due to the charging operations of the EVs. Since the number of EVs in Case 2 is more than Case 1, it causes more power demand for charging. In both cases, the charged energy is used to supply the electrical grid at bus nodes that are determined by the optimization algorithm between 2:40 pm and 6:40 pm. Especially in Case 2, the difference between the minimum and maximum values of load curve is noticeably reduced, which enables the grid to be more efficient and to have a higher capacity utilization rate. In determining the connection points of the EVs, the power demand of the bus and the energy that the EV will consume while reaching the bus are taken into account. Using the values given in Table 2 and Eqs. (18) - (25), the amount of the energy required for the EVs to travel to different bus nodes is calculated as shown in Table 4.

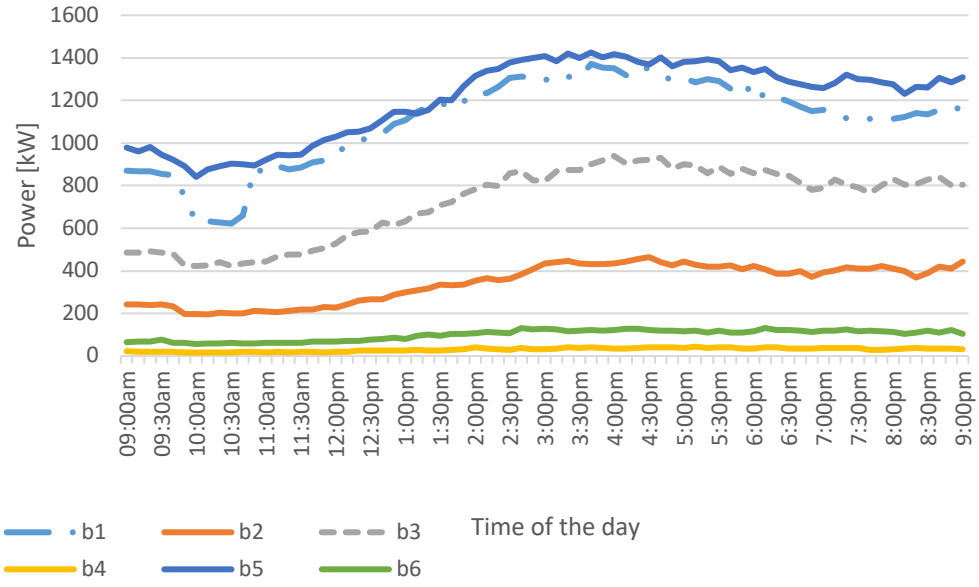

Fig. 3. The power demanded by each bus during the test period.

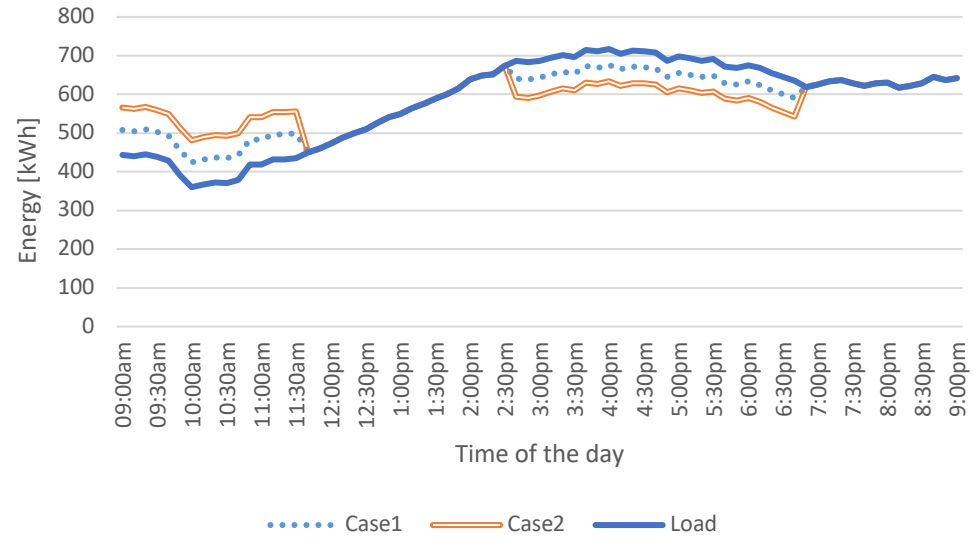

Fig. 4. The energy supplied by the grid during the test period for the Case 1 and Case 2.

Table 4. Energy consumption of the EVs to travel towards the buses

	EV Type-1 (kWh)	EV Type-2 (kWh)
Bus 1	7.082	10.959
Bus 2	6.668	10.335
Bus 3	15.204	23.991
Bus 4	3.230	4.923
Bus 5	10.685	16.567
Bus 6	17.060	26.709

The objective function of the constrained optimization algorithm determines the number of the EVs connected to the buses in order to minimize the energy drawn from the grid during the peak energy period by taking the values in Table 4 into account. The values determined for Case 1 and Case 2 are shown in Fig. 5 (a) and (b), respectively. In Case 1, 15 type-1 EVs are dispatched to Bus 1, Bus 2, Bus 4 and Bus 5 and the quantities of the EVs are 6, 6, 2 and 1, respectively. As each bus has six sockets for these cases, a maximum of six EVs can be connected. In determining the number of EVs going to the bus nodes, the optimization algorithm takes into account the energy demand of each bus node and the amount of energy to be spent to reach these nodes. For Case 1, the maximum number of EVs are connected to Bus 1 and Bus 2. Likewise, for Case 2, the maximum number of EVs are connected to Bus 1, Bus 3, Bus 5 and Bus 6.

After the travel period, EV's battery is charged to be efficient at the peak period. The power demand of consumers is variable throughout the day. The low demand period is the best time to charge EVs. For Case 1 and Case 2, the values of the only four EVs randomly selected are shown in Fig. 6, Fig. 7, Fig. 8 and Fig. 9 for the sake of the brevity.

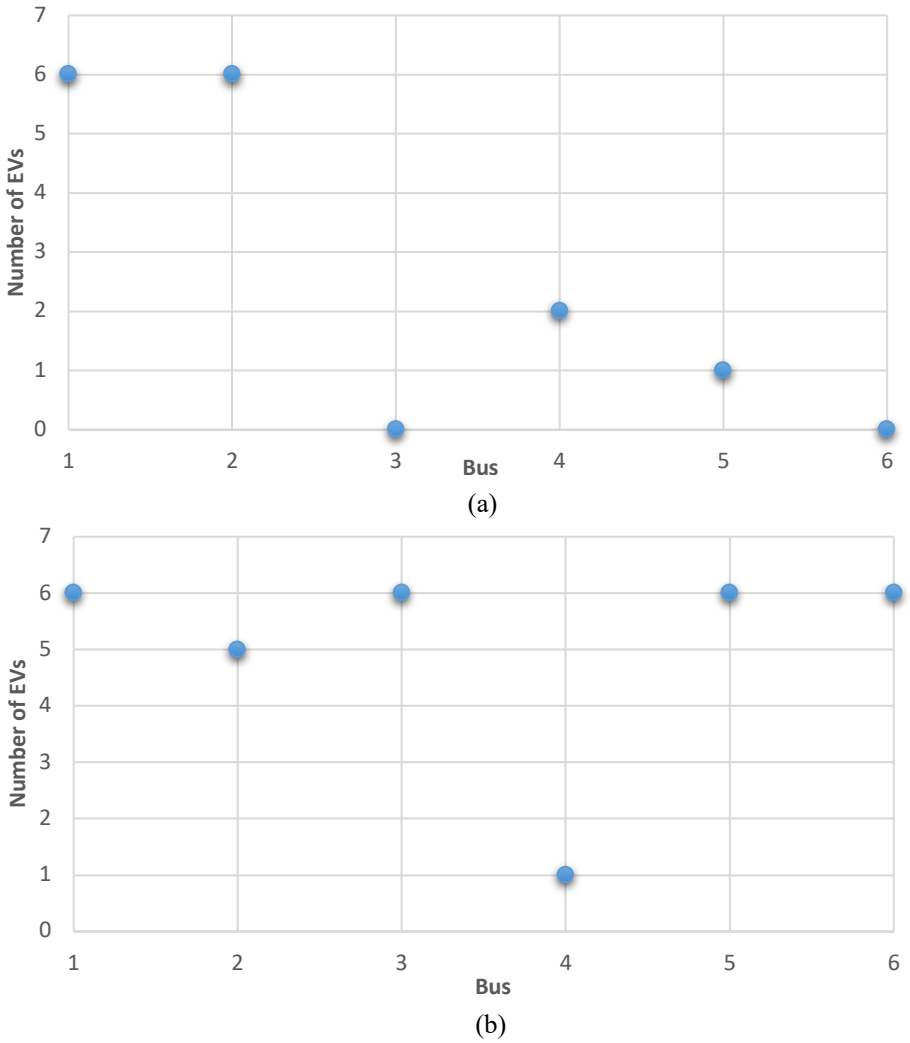

Fig. 5. The number of EVs connected to the buses for (a) Case 1 (b) Case 2.

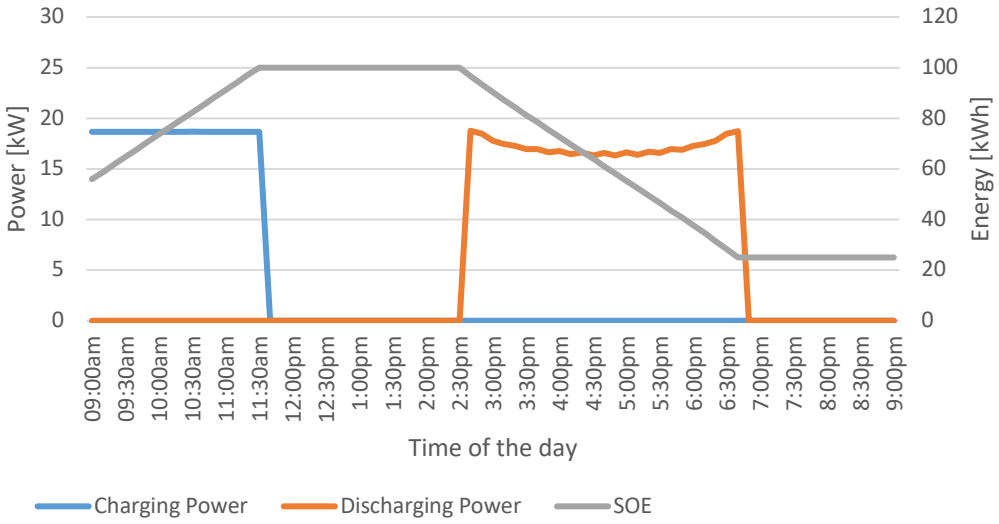

Fig. 6. Battery outputs of EV 5 that is connected to Bus 1 during the test period for Case 1.

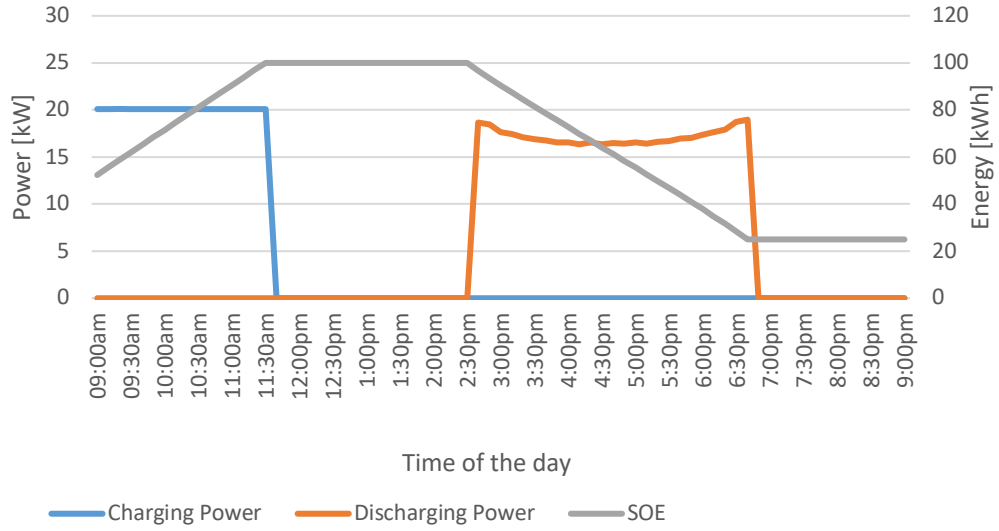

Fig. 7. Battery outputs of EV 14 that is connected to Bus 5 during the test period for Case 1.

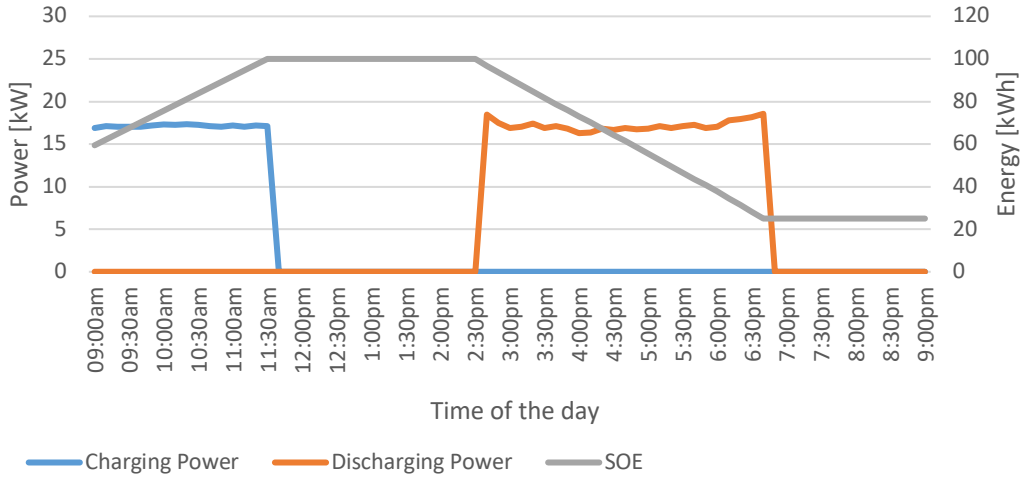

Fig. 8. Battery outputs of EV 19 that is connected to Bus 4 during the test period for Case 2.

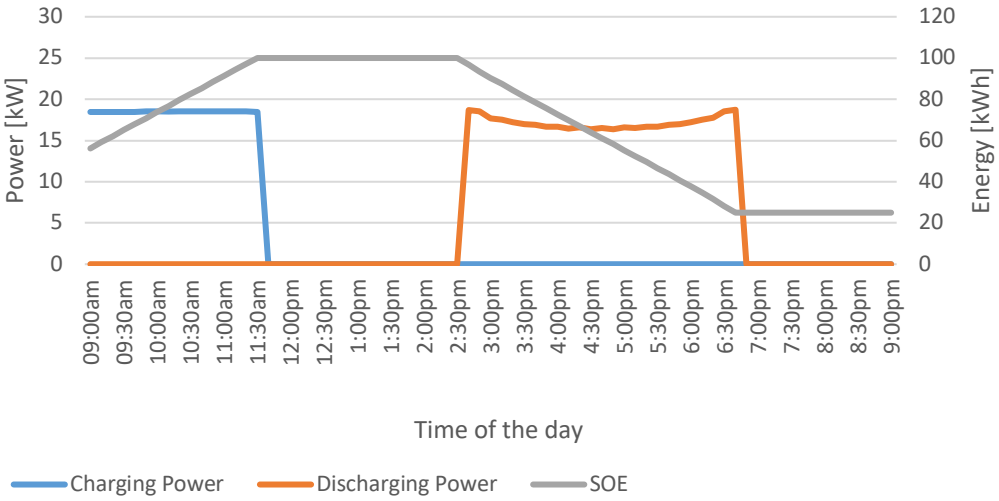

Fig. 9. Battery outputs of EV 15 that is connected to Bus 2 during the test period for Case 2.

Compared to Case 1 and Case 2, the EV type with larger capacity is used for operations in Cases 3 and 4. While the power demand of the consumers remains the same, the change in the specifications of the EV causes great changes in the amount of energy drawn from the grid. The energy supplied by the grid during the test period for Case 3 and Case 4 is shown in Fig. 10. It is obviously observed that quantity of EV is important for economic and reliable system management. In Case 3, it can be said that the optimal operation is possible with the decided quantity of EVs. However, in Case 4, the peak energy period of the curve is changed due to the high energy demand of EVs.

The power demanded, the power the EV can provide and the amount of energy required to travel to any bus have a significant effect on the number of EVs to be connected to the different buses. For Case 3 and Case 4, the distribution of the EV fleet to the buses is shown in Fig. 11 (a) and (b), respectively.

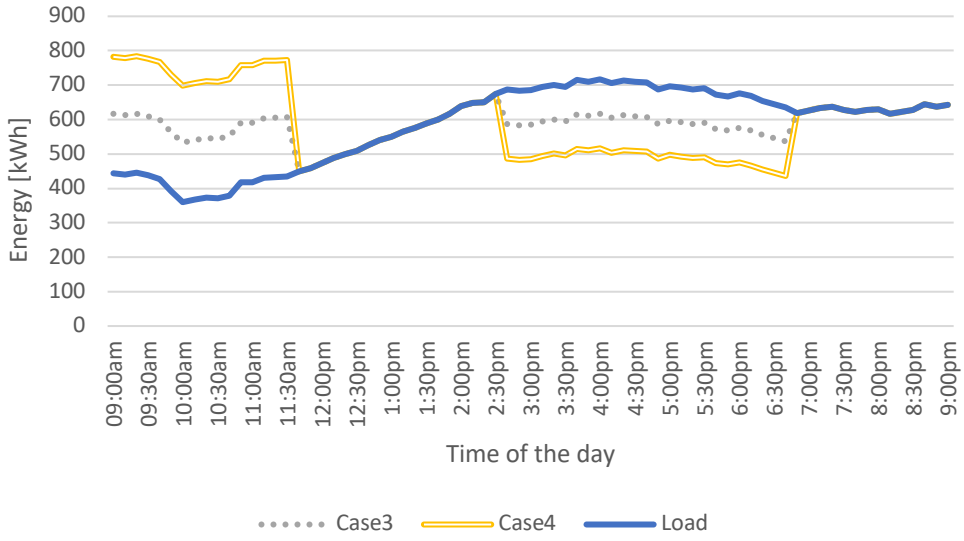

Fig. 10. The energy supplied by the grid during the test period for the Case 3 and Case 4.

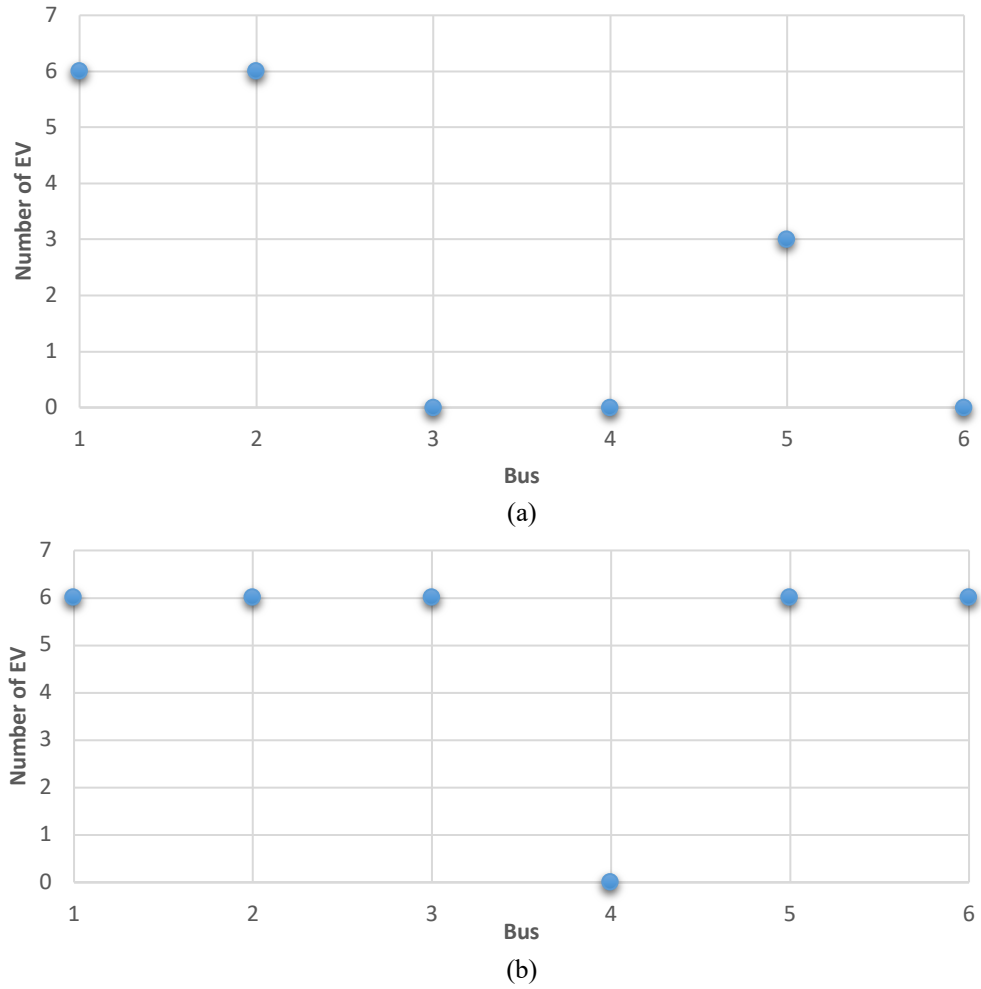

Fig. 11. The number of EVs connected to the buses for (a) Case 3 (b) Case 4.

For Case 3 and Case 4, the battery characteristics of randomly selected EVs are shown in Fig. 12, Fig. 13, Fig. 14 and Fig. 15. Compared to the first two cases, it is seen that more energy is stored due to the large capacity of the battery. In order to charge and discharge the larger capacities in the same time interval, the charging stations with high instantaneous power are used.

For Case 1 and Case 2, the instantaneous charging and discharging powers are around 20kW while for Case 3 and Case 4, these values are around 60kW and 40kW, respectively. Lastly, it can be seen that the increase in the number of EVs reduces the load on the grid. In particular, the number and battery capacity of EVs evaluated in Case 3 achieve greater improvement in the load curve than in the other cases. Besides, when the Peak-to-Average Power Ratio (PAPR) values of all cases are compared, it is seen that Case 3 outperforms the other cases. The calculated PAPR values are 1.1578, 1.1593, 1.1469, 1.3295 and 1.2274 for Case 1, Case 2, Case 3, Case 4 and Load Curve, respectively. The fact that the EV fleet in Case 4 might demand more energy from the grid causes the peak time to change in the load curve. At the same time, due to the higher peak value in Case 4, the largest PAPR value calculated in Case 4. EVs reduce the difference between the minimum and maximum points of the power curve by performing valley filling and peak shaving with charging and discharging operations in different time periods. The flattening of the load curve indicates the

possibility of an increase in the capacity utilization rate. It allows to ensure system reliability and sustainability by avoiding the new investments with high costs. This provides a more efficient system in terms of investment costs and benefits. The energy that the EV supplies to the grid is shown in Table 5 for all cases.

The results obtained show that the EV fleet is used flexibly since it belongs to the distribution company, i.e., it can be used at any time period and in any place with a required capacity, differently from shared ESSs. Therefore, the EV fleet can be managed according to the short-time and seasonal load changes in the form of fleet expansion or contraction. In addition, considering that the capacity and location of the shared ESS are fixed, it is obvious that the proposed system brings an advantage in terms of costs.

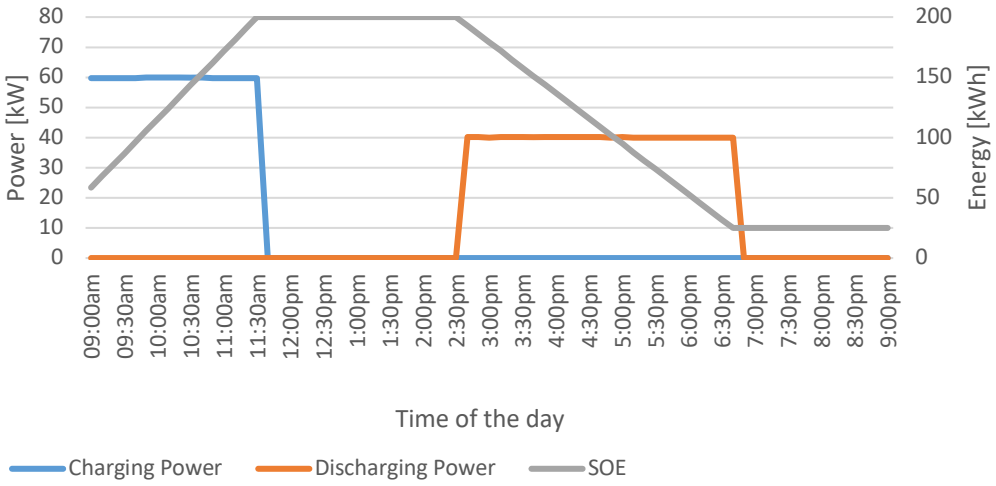

Fig. 12. Battery outputs of EV 8 that is connected to Bus 1 during the test period for Case 3.

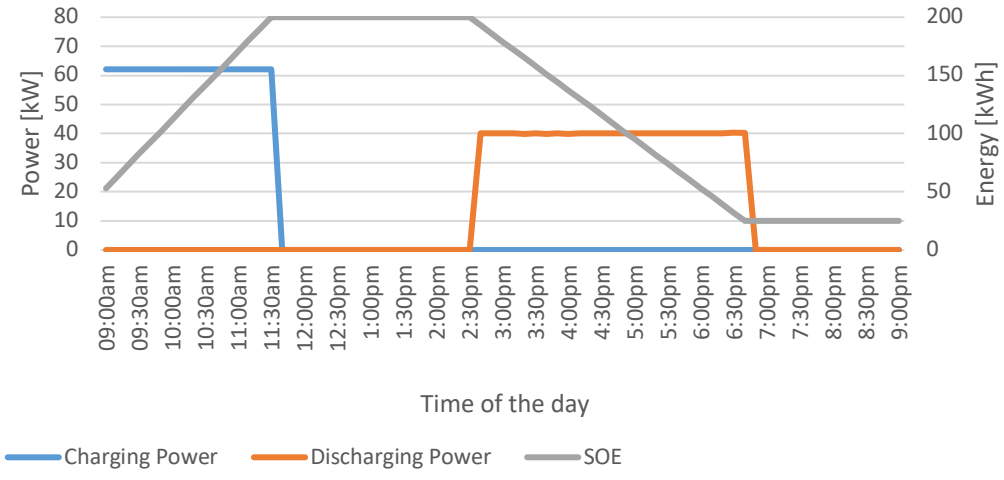

Fig. 13. Battery outputs of EV 6 that is connected to Bus 5 during the test period for Case 3.

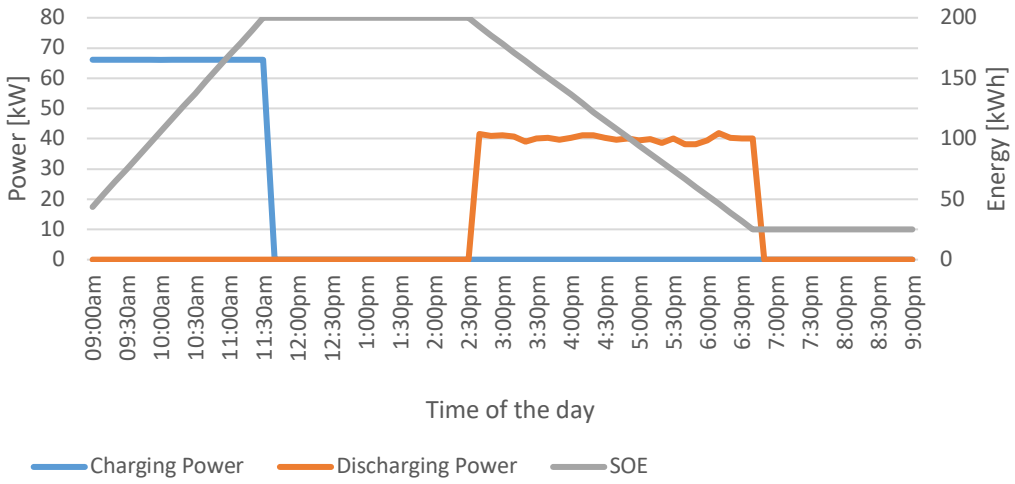

Fig. 14. Battery outputs of EV 17 that is connected to Bus 6 during the test period for Case 4.

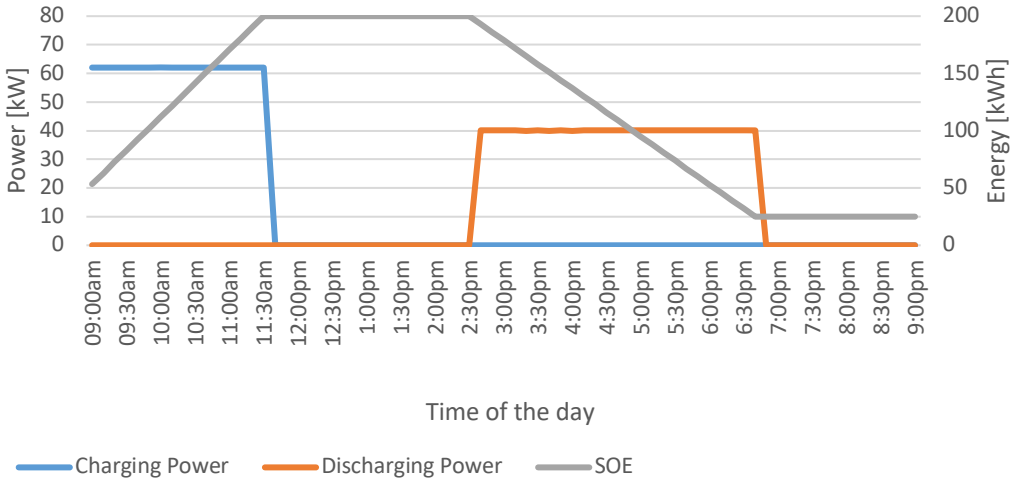

Fig. 15. Battery outputs of EV 12 that is connected to Bus 5 during the test period for Case 4.

Table 5. Energy consumption values

	Energy drawn from grid during peak energy period (kWh)	Energy supplied by EV during peak energy period (kWh)
Case 1	34851.837	739.427
Case 2	33783.087	1624.133
Case 3	33426.837	2406.945
Case 4	30933.166	5000.360
Case 5	30620.773	2340.467

As another important issue, it should be noted that the battery aging and operating costs of the EVs should be taken into account in determining the charge and discharge periods of the EV fleet. Thus, the EV fleet is used only for the time intervals where needed instead of more frequently usage that might also provide some benefits. Moreover, the unnecessary operation of the EVs is prevented since the energy required to travel to a bus and the power demand of the bus are taken into account before any EV is connected to the related bus. Besides, the line losses are reduced as the load demand is supplied from the closest bus thanks to the VfG operations.

In Case 5, in addition to an EV fleet with 15 type-2 EVs, RES and an ESS are added to the network. It is assumed a renewable energy power plant and an ESS are connected to each bus node. The generated power values of the power plants considered are shown in Fig. 16.

Besides, each bus node is equipped with an ESS with a capacity of 400 kWh in Case 5. In order to evaluate the effects of the ESSs on the system, the constraints (29-33) are added to the optimization algorithm where (29) and (30) represent the charge and discharge power constraints, respectively and the SOE of the ESS at each bus node is calculated by Eq (31). Also, the constraints and initial values of SOE are expressed by Eqs. (32) and (33). The energy exchange parameters of the considered ESSs are given in Table 3.

$$0 \le P_{i,t}^{ESS,\mathrm{ch}} \le R_i^{ESS,\mathrm{ch}} \ \forall i,t \tag{29}$$

$$0 \le P_{i,t}^{ESS,dis} \le R_i^{ESS,dis} \ \forall i,t \tag{30}$$

$$\mathrm{SOE}_{\mathrm{i,t}}^{\mathrm{ESS}} = \mathrm{SOE}_{\mathrm{i,(t-1)}}^{\mathrm{ESS}} + \left(\mathrm{CE}^{\mathrm{ESS}} \cdot \mathrm{P}_{\mathrm{i,t}}^{\mathrm{ESS,ch}} - \frac{\mathrm{P}_{\mathrm{i,t}}^{\mathrm{ESS,dis}}}{\mathrm{DE}^{\mathrm{ESS}}} \right) \cdot \Delta \mathrm{T} \ \forall \mathrm{t} \tag{31}$$

$$SOE_i^{ESS,min} \le SOE_{i,t}^{ESS} \le SOE_i^{ESS,max} \ \forall i,t \tag{32}$$

$$SOE_{i,1}^{ESS} = SOE_i^{ESS,ini} \ \forall i \tag{33}$$

The energy drawn from the grid in Case 5 is shown in Fig. 17. Compared to Case 3, which was the best case among the previous cases, there is no significant change in the charging period. However, it is seen in Case 5 that the energy drawn from the grid is less than Case 3, which implies a more effective peak shaving operation. Besides, in this case, the PAPR value is calculated as 1.1727.

The power curves of the charging and discharging operations of the ESSs are shown in Fig. 18 and Fig. 19, respectively. Also, the change in the SOEs of ESSs during the test period is shown in Fig. 20. Except for Bus 4, all the buses use their highest capacity to obtain the maximum operational benefits from the ESSs. In Bus 4, it is seen that less amount of energy is charged and discharged due to the relatively lower load demand.

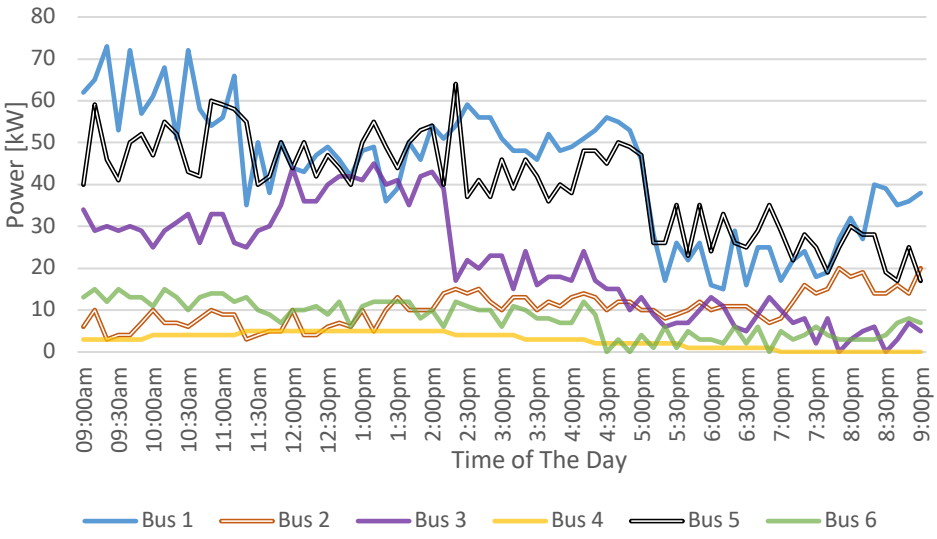

Fig. 16. The power generation of power plants during the test period.

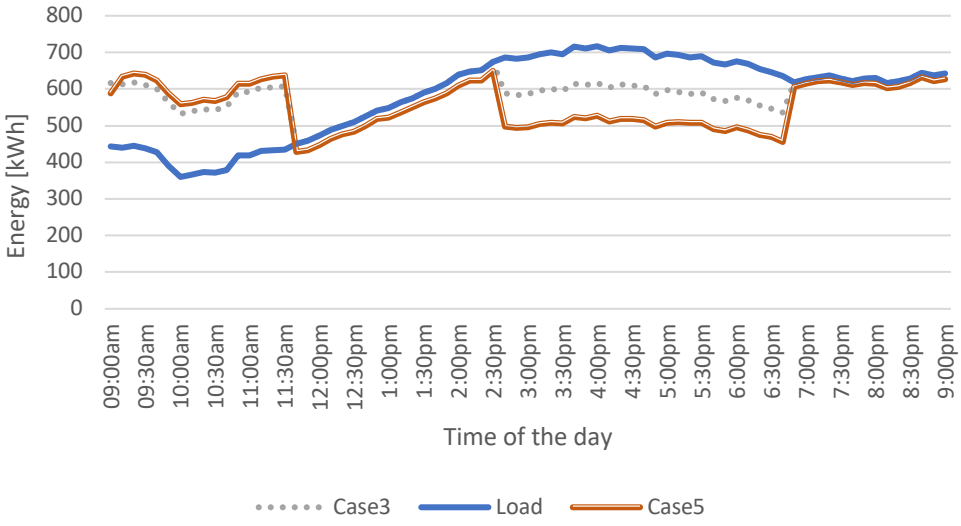

Fig. 17. The energy supplied by the grid during the test period for the Case 3 and Case 5.

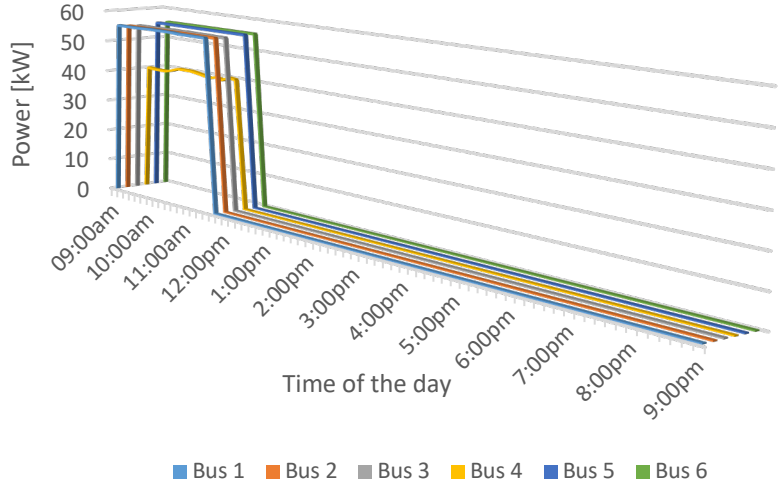

Fig. 18. The charging power of ESSs during the test period for Case 5.

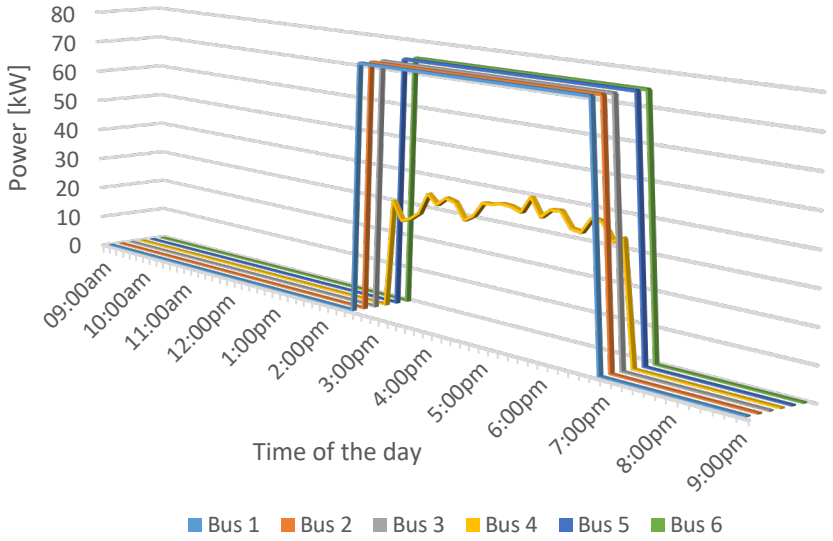

Fig. 19. The discharging power of ESSs during the test period for Case 5.

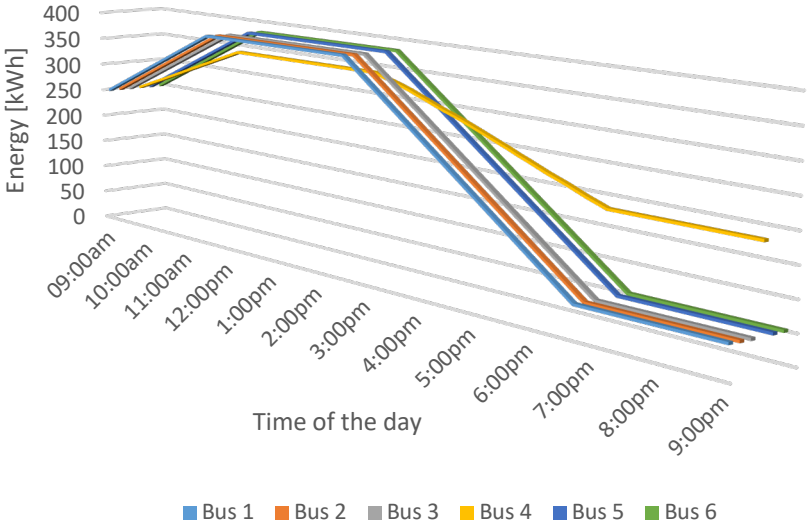

Fig. 20. The change in SOEs of ESSs during the test period in Case 5.

4. Discussion

There are technical, economic, regulatory and social barriers to the development of the V2G technology. In the near future, the developments in the battery structures, charging infrastructures, power network design, data security and communication network technology will facilitate the expansion of V2G operations. From an economic point of view, the decrease in EV purchase and maintenance prices, the charging station installation costs and communication costs will support the spread of the V2G technology. Synchronously with all these technological developments, it is necessary for the legislators to prepare the necessary market laws, and in the social sense, the users who have confidence problems in V2G operations and who have anxiety about running out of battery should be included in the system with incentives [30,31].

The proposed constrained optimization algorithm aims to use EVs as mobile energy storage systems at appropriate times in order to offer a more flexible, safe and efficient grid management. Besides, using EVs in VfG mode prevents the distribution system operator from facing any restrictions on the use of EVs. Due to the constraints imposed by the EV owners in the V2G mode, the required amount of energy and quantity of EV may not be in use during the peak energy period of the electrical grid, which can be stated as the main drawback of the V2G mode. The results prove that the use of EVs in VfG mode in the peak energy period is beneficial in alleviating the overload on the grid.

Besides, in the real applications, distribution system operators already use mobile transformers and mobile batteries in the situations such as planned maintenances, temporary capacity increases, system failures and natural disasters. Motivated by this fact, it can be foreseen that the VfG technology including mobile batteries with different capacities would be used by the distribution system operators to provide further operational benefits to the system operations. Furthermore, the widespread use of EVs and increase in the charging and service points would make the VfG technology one of the most applicable and effective options in near future in the system operations during especially the peak load demand periods.

5. Conclusions

The constrained optimization algorithm minimizes the objective function by taking into account the energy demand of each bus node and the amount of energy required to travel between them. The EV fleet is dispatched to the bus nodes determined by the algorithm, not exceeding the maximum number of sockets. The best results are observed in Case 3 were 15 type-2 EVs each with 200-kWh batteries are included. Thanks to the valley filling and peak shaving operation of the EVs, the PAPR value for the load curve decreased by 6.56% in Case 3. While there is a double difference between the minimum and maximum points in the load curve, it is seen that the difference almost disappears and the curve becomes horizontal. Since the EVs in Case 4 have the highest storage capacity, it provides the best discharging power performance that is 5000 kWh during the peak energy period. The large amount of energy drawn from the grid to charge the EVs shifts the load curve upwards and causes the peak time to change. Thus, the number and characteristics of EVs should be determined by considering the energy consumption between the parking area and the bus node, and the load characteristics of the system.

As a future study, additional results can be obtained using the grid with different load profiles and the fleet of EVs with various battery capacities by also improving the designed algorithm. In addition, the most suitable operating conditions can be determined by taking the purchase, operation, maintenance and repair costs of the EVs into account.

ACKNOWLEDGEMENT

This work of A. Taşcıkaraoğlu is supported by the Turkish Academy of Sciences (TUBA) within the framework of the Distinguished Young Scientist Award Program (GEBIP).

REFERENCES

[1] L. Cozzi et al., "World Energy Outlook 2020," vol. 2050, no. October, pp. 1–461, 2020.

[2] EIA, "International Energy Outlook 2019," U.S. Energy Inf. Adm., September, no. 09, pp. 25–150, 2019.

[3] EIA., "International Energy Outlook 2016," U.S. Energy Inf. Adm., May, pp. 1–276, 2016.

[4] I. S. Bayram, A. Tajer, M. Abdallah, and K. Qaraqe, "Capacity Planning Frameworks for Electric Vehicle Charging Stations With Multiclass Customers," IEEE Trans. Smart Grid, vol. 6, no. 4, pp. 1934–1943, 2015.

[5] R. A. Verzijlbergh, M. O. W. Grond, Z. Lukszo, J. G. Slootweg, and M. D. Ilic, "Network impacts and cost savings of controlled EV charging," IEEE Trans. Smart Grid, vol. 3, no. 3, pp. 1203–1212, 2012.

[6] T. Lehtola and A. Zahedi, "Electric vehicle to grid for power regulation: A review," 2016 IEEE Int. Conf. Power Syst. Technol. POWERCON 2016, pp. 1–6, 2016.

[7] N. Naik and C. Vyjayanthi, "Optimization of Vehicle-to-Grid (V2G) Services for Development of Smart Electric Grid: A Review," pp. 1–6, 2021.

[8] E. Alghsoon, A. Harb, and M. Hamdan, "Power Quality and Stability Impacts," 8th Int. Renew. Energy Congr. (IREC 2017) Power, no. Irec, pp. 7–12, 2017.

[9] C. Xu, Y. Wan, S. Zhang and W. He, "Optimal configuration of ES capacity under the access of EV in V2G mode," 40th Chinese Control Conf., pp. 1862–1868, 2021.

[10] S. Das, P. Thakur, A. K. Singh, and S. N. Singh, "Optimal management of vehicle-to-grid and grid-to-vehicle strategies for load profile improvement in distribution system," J. Energy Storage, vol. 49, no. September 2021, p. 104068, 2022.

[11] M. A. Hannan et al., "Vehicle to grid connected technologies and charging strategies: Operation, control, issues and recommendations," J. Clean. Prod., vol. 339, no. August 2021, p. 130587, 2022.

[12] S. S. Ravi and M. Aziz, "Utilization of Electric Vehicles for Vehicle-to-Grid Services: Progress and Perspectives," Energies, vol. 15, no. 2, 2022.

[13] M. A. Hannan et al., "Vehicle to grid connected technologies and charging strategies: Operation, control, issues and recommendations," J. Clean. Prod., vol. 339, no. August 2021, p. 130587, 2022.

[14] Y. Qin et al., "Lithium-ion batteries under pulsed current operation to stabilize future grids," Cell Reports Phys. Sci., vol. 3, no. 1, p. 100708, 2022.

[15] J. Qi, L. Li, and G. Lei, "Economic Operation of a Workplace EV Parking Lot under Different Operation Modes," Proc. 2021 31st Australas. Univ. Power Eng. Conf. AUPEC 2021, 2021.

[16] E. L. Karfopoulos, K. A. Panourgias, and N. D. Hatziargyriou, "Distributed Coordination of Electric Vehicles providing V2G Regulation Services," IEEE Trans. Power Syst., vol. 31, no. 4, pp. 2834–2846, 2016.

[17] D. Guo and C. Zhou, "Realistic modeling of vehicle-to-grid in an enterprise parking lot: A stackelberg game approach," 2018 IEEE Texas Power Energy Conf. TPEC 2018, vol. 2018-Febru, pp. 1–6, 2018.

[18] U. ur Rehman, M. Riaz, and M. Y. Wani, "A robust optimization method for optimizing day-ahead operation of the electric vehicles aggregator," Int. J. Electr. Power Energy Syst., vol. 132, no. May, p. 107179, 2021.

[19] B. Tepe, J. Figgener, S. Englberger, D. U. Sauer, A. Jossen, and H. Hesse, "Optimal pool composition of commercial electric vehicles in V2G fleet operation of various electricity markets," Appl. Energy, vol. 308, no. July 2021, p. 118351, 2022.

[20] S. Guo et al., "A multi-level vehicle-to-grid optimal scheduling approach with EV economic dispatching model," Energy Reports, vol. 7, pp. 22–37, 2021.

[21] S. Das, P. Acharjee, and A. Bhattacharya, "A Comprehensive Planning and Analysis of Coordinated Charging Scheduling for On-Road Electric Vehicles," 2021 IEEE 4th Int. Conf. Comput. Power Commun. Technol. GUCON 2021, pp. 1–6, 2021.

[22] W. Wei, F. Liu, and S. Mei, "Charging Strategies of EV Aggregator Under Renewable Generation and Congestion: A Normalized Nash Equilibrium Approach," IEEE Trans. Smart Grid, vol. 7, no. 3, pp. 1630–1641, 2016.

[23] W. Zhong, R. Yu, Y. Zhang, J. Kang, H. Zhang, and S. Xie, "Dynamic demand balance in vehicle-to-grid mobile energy networks," IEEE Int. Conf. Commun., vol. 2015-Septe, pp. 5589–5594, 2015.

[24] M. Rahmani-Andebili, "Vehicle-for-grid (VfG): A mobile energy storage in smart grid," IET Gener. Transm. Distrib., vol. 13, no. 8, pp. 1358–1368, 2019.

[25] M. Baradar and M. R. Hesamzadeh, "AC power flow representation in conic format," IEEE Trans. Power Syst., vol. 30, no. 1, pp. 546–547, 2015.

[26] I. Şengör, A. K. Erenoğlu, O. Erdinç, A. Taşcikaraoğlu, and J. P. S. Catalão, "Day-ahead charging operation of electric vehicles with on-site renewable energy resources in a mixed integer linear programming framework," IET Smart Grid, vol. 3, no. 3, pp. 367–375, 2020.

[27] J. A. P. L. Garcia-Val, Rodrigole, Ed., Power Electronics and Power Systems. Springer, 2013.

[28] A. Taşcıkaraoğlu, "Economic and operational benefits of energy storage sharing for a neighborhood of prosumers in a dynamic pricing environment," Sustain. Cities Soc., vol. 38, no. November 2017, pp. 219–229, 2018.

[29] Tesla Cybertruck Tri Motor Specifications. Available Online: https://ev-database.org/car/1250/Tesla-Cybertruck-Tri-Motor (accessed on 29 July 2022)

[30] L. Noel, Z. de R. Gerardo, J. Kester, and B. K. Sovacool, “Vehicle-to-grid: A sociotechnical transition beyond electric mobility,” Cham, Switzerland: Palgrave Macmillan, 2019.

[31] E. Crisostomi, R. Shorten, Stüdli Sonja, and F. Wirth, “Electric and plug-in Hybrid Vehicle Networks: Optimization and Control,” CRC Press, 2018.